Commun. Comput. Phys.
doi: 10.4208/cicp.231014.110416a

Vol. **20**, No. 5, pp. 1313-1339
November 2016

An Energy-Preserving Wavelet Collocation Method for General Multi-Symplectic Formulations of Hamiltonian PDEs

Yuezheng Gong and Yushun Wang*

Jiangsu Key Laboratory of NSLSCS, School of Mathematical Sciences, Nanjing Normal University, Nanjing 210023, P.R. China.

Received 23 October 2014; Accepted (in revised version) 11 April 2016

Abstract. In this paper, we develop a novel energy-preserving wavelet collocation method for solving general multi-symplectic formulations of Hamiltonian PDEs. Based on the autocorrelation functions of Daubechies compactly supported scaling functions, the wavelet collocation method is conducted for spatial discretization. The obtained semi-discrete system is shown to be a finite-dimensional Hamiltonian system, which has an energy conservation law. Then, the average vector field method is used for time integration, which leads to an energy-preserving method for multi-symplectic Hamiltonian PDEs. The proposed method is illustrated by the nonlinear Schrödinger equation and the Camassa-Holm equation. Since differentiation matrix obtained by the wavelet collocation method is a cyclic matrix, we can apply Fast Fourier transform to solve equations in numerical calculation. Numerical experiments show the high accuracy, effectiveness and conservation properties of the proposed method.

AMS subject classifications: 65M06, 65M70, 65T50, 65Z05

Key words: Energy-preserving, average vector field method, wavelet collocation method, nonlinear Schrödinger equation, Camassa-Holm equation.

1 Introduction

A numerical method which can preserve one or more physical/geometric properties of the system exactly is called geometric or structure-preserving integrators. As geometric integration has gained remarkable success in the numerical analysis of ODEs [1, 2], it is believable to extend the idea of geometric integration to significant PDEs. Many conservative PDEs, for instance the sine-Gordon (SG) equation, the nonlinear Schrödinger

*Corresponding author. *Email addresses:* gyz8814@163.com (Y. Gong), wangyushun@njnu.edu.cn (Y. Wang)

 ©2016 Global-Science Press

https://doi.org/10.4208/cicp.231014.110416a Published online by Cambridge University Press

(NLS) equation, the Korteweg-de Vries (KdV) equation, the Camassa-Holm (CH) equation, the Maxwell's equations and so on can be rewritten as multi-symplectic Hamiltonian system, which has the properties of multi-symplectic structure, energy and momentum conservation laws [3–5]. To inherit the multi-symplectic structure, many multi-symplectic methods [6–9] are developed in recent years. For more details in applications, please refer to review articles [10, 11] and references therein. Except the multi-symplectic conservation law, multi-symplectic Hamiltonian system also has the energy conservation law. The conservation of energy is a crucial property of mechanical systems and plays an important role in the study of properties of solutions [12, 13]. It is valuable to expect that energy-preserving discretizations for conservative PDEs will produce richer information on the discrete systems. Li and Vu-Quoc [14] gave a historical survey of energy-preserving methods for PDEs and their applications, especially to nonlinear stability. Energy-preserving methods [15–19] have successfully made many applications. However, these methods have an ad hoc character and are not completely systematic either in their derivation or in their applicability; in contrast, our method discussed here is completely systematic, applied to a huge class of conservation PDEs.

Recently, wavelet-based numerical methods become increasingly popular as they combine the advantages of both spectral method and finite difference method (FDM) [20–22]. Compared with spectral method, wavelet-based methods have good spatial localization and generate a sparse space differentiation matrix, and compared with FDM, wavelet-based methods have good spectral localization and higher order of accuracy. The wavelet-based algorithms can be roughly classified into two categories: wavelet-Galerkin and wavelet collocation. In [23] and [24], Daubechies' compactly supported orthogonal wavelets and second-generation wavelets are proposed to combine with symplectic schemes to construct multiresolution symplectic solvers for wave propagation problems and the method is of wavelet-Galerkin type. However, it is very difficult to deal with nonlinear problems, as it needs the passage between wavelet coefficients and physical space. In order to overcome this difficulty, a wavelet collocation method is proposed in [25], in which the autocorrelation functions of Daubechies compactly supported scaling functions are shown to have the merits of symmetry and nice interpolation properties, and so no extra computation is required for the passage between wavelet coefficients and physical space. Based on the autocorrelation functions of Daubechies compactly supported scaling functions, the symplectic wavelet collocation method and the multi-symplectic wavelet collocation method are developed for Hamiltonian PDEs with periodic boundary conditions in [26] and [27], respectively, in which numerical experiments illustrate the remarkable behavior of the methods.

The average vector field (AVF) method is first written down in [28] and identified as energy-preserving and as a B-series method in [29]. For ordinary differential equation

$$\dot{y} = f(y), \quad y \in \mathbb{R}^d, \tag{1.1}$$

https://doi.org/10.4208/cicp.231014.110416a Published online by Cambridge University Press

the AVF method is the map $y \longmapsto y'$ defined by

$$\frac{y'-y}{\tau} = \int_0^1 f\left((1-\xi)y+\xi y'\right) d\xi, \tag{1.2}$$

where τ is the time step. The AVF method (1.2) is affine-covariant, self-adjoint, and of second order [30]. When f is Hamiltonian with respect to a constant symplectic structure, i.e., $f = \Omega^{-1}\nabla H$ with Ω a nonsingular, skew-symmetric matrix, the AVF method preserves the Hamiltonian H. Note that the key of the AVF method is to integrate the integration of (1.2) exactly. As we know, the above integration can be integrated exactly when f is a polynomial. In [30] and [31], authors apply high-order Runge-Kutta methods and collocation methods to approximate the integration of (1.2) and obtain energy-preserving methods. By using the AVF method, Ref. [32] gave a class of systematic energy-preserving methods based on symplectic formulation of Hamiltonian PDEs. Basic idea of the methods is to first discretize PDEs with an uniform spatial-discretization resulting in a large system of Hamiltonian ODEs. Then, the resulting ODEs are integrated by the AVF method. Recently, we started from general multi-symplectic formulations of Hamiltonian PDEs and utilized the AVF method to construct a local energy-preserving method and a local momentum-preserving method [33].

The purpose of this paper is to construct a new class of systematic energy-preserving methods for multi-symplectic formulations of Hamiltonian PDEs. Based on the autocorrelation functions of Daubechies compactly supported scaling functions, the wavelet collocation method is conducted for spatial discretization of multi-symplectic PDEs. The semi-discrete system is shown to be a finite-dimensional Hamiltonian system, which has an energy conservation law. Then, the AVF method is used for time integration, which leads to an energy-preserving wavelet collocation method (EPWCM) for multi-symplectic Hamiltonian PDEs. To our knowledge, it has not been reported that the wavelet collocation method is applied to construct energy-preserving schemes for the multi-symplectic PDEs. The proposed method is illustrated by the NLS equation and the CH equation. Since differentiation matrix obtained by the wavelet collocation method is a cyclic matrix [26, 34], we can apply Fast Fourier transform (FFT) to solve equations in numerical calculation. Numerical experiments show the high accuracy, effectiveness and conservation properties of the proposed method. The proposed method can be used for general Hamiltonian PDEs. Thus, the SG equation, the NLS equation, the KdV equation, the CH equation, the Maxwell's equations and so on can be integrated by the proposed method.

The rest of this paper is organized as follows: in Section 2, multi-symplectic PDEs and autocorrelation functions are briefly introduced, then an EPWCM is developed for multi-symplectic PDEs. The proposed method is applied to derive energy-preserving algorithm for the NLS equation and the CH equation in Sections 3 and 4 respectively. To demonstrate the accuracy and capability of the method, numerical experiments for the NLS equation and the CH equation are reported in Sections 5 and 6 respectively. Conclusions are given in Section 7.

https://doi.org/10.4208/cicp.231014.110416a Published online by Cambridge University Press

2 Energy-preserving wavelet collocation method for multi-symplectic PDEs

In this section, multi-symplectic PDEs and autocorrelation functions are briefly introduced, then a novel energy-preserving wavelet collocation method is developed for multi-symplectic PDEs.

2.1 Multi-symplectic PDEs

A wide range of PDEs can be written as a multi-symplectic system

$$\mathbf{M}\mathrm{z}_t+\mathbf{K}\mathrm{z}_x=\nabla_{\mathrm{z}}S(\mathrm{z}),\quad \mathrm{z}\in\mathbb{R}^d,\ (x,t)\in\mathbb{R}^2, \tag{2.1}$$

where $\mathbf{M}$ and $\mathbf{K}$ are two skew-symmetric matrices and $S:\mathbb{R}^d\to\mathbb{R}$ is a scalar-valued smooth function. The above system has three local conservation laws [35, 36], namely multi-symplectic conservation law

$$\partial_t\omega+\partial_x\kappa=0,\quad \omega=d\mathrm{z}\wedge\mathbf{M}_+d\mathrm{z},\quad \kappa=d\mathrm{z}\wedge\mathbf{K}_+d\mathrm{z}, \tag{2.2}$$

local energy conservation law (LECL)

$$E_t+F_x=0,\quad E=S(\mathrm{z})+\mathrm{z}_x^T\mathbf{K}_+\mathrm{z},\quad F=-\mathrm{z}_t^T\mathbf{K}_+\mathrm{z}, \tag{2.3}$$

local momentum conservation law (LMCL)

$$I_t+G_x=0,\quad G=S(\mathrm{z})+\mathrm{z}_t^T\mathbf{M}_+\mathrm{z},\quad I=-\mathrm{z}_x^T\mathbf{M}_+\mathrm{z}, \tag{2.4}$$

where $\mathbf{M}_+$ and $\mathbf{K}_+$ satisfy

$$\mathbf{M}=\mathbf{M}_+-\mathbf{M}_+^T,\quad \mathbf{K}=\mathbf{K}_+-\mathbf{K}_+^T.$$

Note that the splitting of $\mathbf{M}$ and $\mathbf{K}$ is to deduce efficiently correct expressions of energy and momentum in physics. For periodic boundary conditions, the local conservation laws can be integrated in x-direction to obtain global conservation of energy and momentum.

2.2 Autocorrelation functions

A Daubechies scaling function $\phi(x)$ with M non-vanishing "filter coefficients"(in short, DM) satisfies the scaling relation:

$$\phi(x)=\sqrt{2}\sum_{k=0}^{M-1}h_k\phi(2x-k), \tag{2.5}$$

https://doi.org/10.4208/cicp.231014.110416a Published online by Cambridge University Press

where M is a positive even number and $\{h_k\}_{k=0}^{M-1}$ are non-vanishing "filter coefficients". Define the autocorrelation function $\theta(x)$ of $\phi(x)$ (in short, ADM) as

$$\theta(x)=\big(\phi*\phi(-\cdot)\big)(x)=\int\phi(t)\phi(t-x)dt. \tag{2.6}$$

Suppose that V_j is the linear span of $\{\theta_{j,k}(x)=2^{j/2}\theta(2^jx-k),k\in\mathbb{Z}\}$, then $(V_j)_{j\in\mathbb{Z}}$ forms a multiresolution analysis where $\theta(x)$ plays the role of (nonorthonormal) scaling function. The values of the function $\theta(x)$ and its derivatives at integer points can be obtained by solving an eigenvalue problem, see [20,22] for more details.

The function $\theta(x)$ has interpolation property:

$$\theta(l)=\int\phi(t)\phi(t-l)dt=\delta_{0,l},\quad l\in\mathbb{Z}. \tag{2.7}$$

An interpolation operator on V_j (with the space step $h=2^{-j}$) can be defined as

$$I_ju(x)=2^{-\frac{j}{2}}\sum_{k\in\mathbb{Z}}u(2^{-j}k)\theta_{j,k}(x)=\sum_{k\in\mathbb{Z}}u(2^{-j}k)\theta(2^jx-k). \tag{2.8}$$

2.3 Energy-preserving wavelet collocation method for multi-symplectic PDEs

Wavelet collocation method based on the autocorrelation function $\theta(x)$ is used for spatial discretization. The obtained semi-discrete system is shown to be a finite-dimensional Hamiltonian system, which has an energy conservation law. Then, the AVF method is employed for time integration, which leads to an energy-preserving method for multi-symplectic Hamiltonian PDEs.

2.3.1 Wavelet collocation method for spatial discretization

In this section, wavelet collocation method is used for spatial discretization for the multi-symplectic PDEs (2.1) with periodic boundary conditions. We use the autocorrelation function ADM in the framework of a collocation method.

Consider the multi-symplectic PDEs (2.1) with the spatial domain being $[x_L,x_R]$, where x_L and x_R are integers. We set $\mathrm{z}=(u_1,u_2,\cdots,u_d)^T$ and use the interpolation operator (2.8) to approximate $u_i(x,t)$ $(i=1,2,\cdots,d)$. For a fixed scale $J=$ constant, we approximate function $u_i(x,t)$ by an interpolation operator $I_Ju_i(x,t)$, which interpolates $u_i(x,t)$ at collocation points $x_l=x_L+l/2^J$, for $l=0,1,\cdots,N-1$, $N=(x_R-x_L)\cdot2^J$. The interpolation operator $I_Ju_i(x,t)$ has the form

$$I_Ju_i(x,t)=\sum_{m\in\mathbb{Z}}u_{i_m}\theta\big(2^Jx-(x_L\cdot2^J+m)\big), \tag{2.9}$$

where $u_{i_m}=u_i(x_m,t)$ and $u_{i_m}=u_{i_{m+N}}$, $m\in\mathbb{Z}$. According to the interpolation property (2.7), we have $I_Ju_i(x_l,t)=u_i(x_l,t)$.

https://doi.org/10.4208/cicp.231014.110416a Published online by Cambridge University Press

Applying the wavelet collocation method for spatial discretization of multi-symplectic system (2.1), we obtain

$$\mathbf{M}(\mathrm{z}_l)_t+\mathbf{K}(I_J\mathrm{z})_x|_{x=x_l}=\nabla_{\mathrm{z}}S(\mathrm{z}_l), \tag{2.10}$$

where $I_J\mathrm{z}=(I_Ju_1,I_Ju_2,\cdots,I_Ju_d)^T$ and $\mathrm{z}_l=(u_{1_l},u_{2_l},\cdots,u_{d_l})^T$.

To obtain the equations for z_l, the crucial step is to express the first-order spatial partial derivatives at collocation points x_l in terms of the values z_l. Making once differential with (2.9) and evaluating the resulting expressions at collocation points, we obtain

$$\frac{\partial I_Ju_i(x,t)}{\partial x}\Big|_{x_l}=\sum_{m=l-(M-1)}^{l+M-1}u_{i_m}\cdot 2^J\theta'(l-m)=(B_1U_i)_l, \tag{2.11}$$

where $U_i=(u_{i_0},u_{i_1},\cdots,u_{i_{N-1}})^T$ and B_1 is an $N\times N$ matrix with elements

$$(B_1)_{l,m}=\begin{cases}2^J\theta'(l-m), & -M+1\le l-m\le M-1;\\ 2^J\theta'(-k), & l-m=N-k,\ 1\le k\le M-1;\\ 2^J\theta'(k), & m-l=N-k,\ 1\le k\le M-1;\\ 0, & \text{otherwise.}\end{cases} \tag{2.12}$$

The properties of space differentiation matrix have already been analyzed in detail in [26]. Here we note that B_1 is skew-symmetric.

Combining (2.10) with the differentiation matrix B_1, we obtain the wavelet collocation discretization for the multi-symplectic PDEs (2.1)

$$\mathbf{M}\frac{d}{dt}\mathrm{z}_l+\mathbf{K}\sum_{m=0}^{N-1}(B_1)_{l,m}\mathrm{z}_m=\nabla_{\mathrm{z}}S(\mathrm{z}_l),\quad l=0,1,\cdots,N-1, \tag{2.13}$$

which is equivalent to the following compact form

$$(I_N\otimes\mathbf{M})\frac{d}{dt}\mathrm{Z}+(B_1\otimes\mathbf{K})\mathrm{Z}=\nabla_{\mathrm{Z}}\overline{S}(\mathrm{Z}), \tag{2.14}$$

where I_N is the $N\times N$ identity matrix, $\otimes$ means Kronecker inner product, $\mathrm{Z}=(\mathrm{z}_0^T,\mathrm{z}_1^T,\cdots,\mathrm{z}_{N-1}^T)^T$, and $\overline{S}(\mathrm{Z})=\sum_{l=0}^{N-1}S(\mathrm{z}_l)$. Since B_1 and $\mathbf{K}$ are skew-symmetric, $B_1\otimes\mathbf{K}$ is symmetric, the semi-discrete system (2.14) can be written as

$$(I_N\otimes\mathbf{M})\frac{d}{dt}\mathrm{Z}=\nabla_{\mathrm{Z}}H(\mathrm{Z}), \tag{2.15}$$

where $H(\mathrm{Z})=\overline{S}(\mathrm{Z})-\frac{1}{2}\mathrm{Z}^T(B_1\otimes\mathbf{K})\mathrm{Z}$. The discrete total energy of multi-symplectic system (2.1) can be defined as

$$\mathcal{E}(t)=hH(\mathrm{Z}). \tag{2.16}$$

https://doi.org/10.4208/cicp.231014.110416a Published online by Cambridge University Press

Remark 2.1. $H(Z)$ can also be written as

$$H(Z)=\overline{S}(Z)-Z^T(B_1\otimes\mathbf{K}_+)Z=\overline{S}(Z)+Z^T(B_1\otimes\mathbf{K}_+^T)Z, \tag{2.17}$$

which is corresponding to the discrete total energy of Eq. (2.3).

Theorem 2.1. *The wavelet collocation semi-discretization* (2.15) *has the total energy conservation law*

$$\frac{d}{dt}\mathcal{E}(t)=0. \tag{2.18}$$

Proof. Since $I_N\otimes\mathbf{M}$ is antisymmetric, taking inner product with $\frac{d}{dt}Z$ on both sides of (2.15), we obtain

$$0=\left(\frac{d}{dt}Z\right)^T\nabla_Z H(Z)=\frac{d}{dt}H(Z).$$

Therefore, the total energy conservation law (2.18) holds. □

2.3.2 Average vector field method for temporal discretization

Since matrix $I_N\otimes\mathbf{M}$ is usually singular, the semi-discrete system (2.15) is algebraic differential equations, and it is also a gradient system. Therefore, the key of constructing energy-preserving method is to apply a discrete gradient method for the semi-discrete system (2.15). Here the AVF method, as a special discrete gradient method [28], is employed for temporal discretization.

We discretize (2.15) with the AVF method and obtain the energy-preserving wavelet collocation method (EPWCM) for the multi-symplectic PDEs (2.1)

$$(I_N\otimes\mathbf{M})\frac{Z^{n+1}-Z^n}{\tau}=\int_0^1\nabla_Z H\big((1-\xi)Z^n+\xi Z^{n+1}\big)d\xi. \tag{2.19}$$

Note that the integration of (2.19) can be integrated exactly when H is a polynomial. In practical application, the scheme (2.19) can be simplified by eliminating some values (see Section 3 and Section 4).

Theorem 2.2. *The EPWCM* (2.19) *possesses the discrete total energy conservation law*

$$\mathcal{E}^{n+1}=\mathcal{E}^n, \tag{2.20}$$

where $\mathcal{E}^n=hH(Z^n)$.

Proof. Since $I_N\otimes\mathbf{M}$ is antisymmetric, taking inner product with $Z^{n+1}-Z^n$ on both sides of (2.19), we have

$$\begin{aligned}0&=(Z^{n+1}-Z^n)^T\int_0^1\nabla_Z H\big((1-\xi)Z^n+\xi Z^{n+1}\big)d\xi\\&=\int_0^1\frac{d}{d\xi}H\big((1-\xi)Z^n+\xi Z^{n+1}\big)d\xi\\&=H(Z^{n+1})-H(Z^n).\end{aligned}$$

Therefore, the discrete total energy conservation law (2.20) holds. □

https://doi.org/10.4208/cicp.231014.110416a Published online by Cambridge University Press

Remark 2.2. Since differentiation matrix B_1 is a cyclic matrix [26,34], we have

$$B_1 = F_N^{-1} diag(F_N b) F_N, \tag{2.21}$$

where F_N is discrete Fourier transform with elements $(F_N)_{j,n} = W_N^{-jn}$, $W_N = e^{i2\pi/N}$, F_N^{-1} is inverse discrete Fourier transform with elements $(F_N^{-1})_{j,n} = \frac{1}{N} W_N^{jn}$ and b is the first column of B_1.

Remark 2.3. By the relation (2.21), we can evaluate the derivatives by using the FFT algorithm instead of differentiation matrix B_1 in $\mathcal{O}(N\log_2 N)$ operations rather than $\mathcal{O}(N^2)$ operations.

Remark 2.4. The discrete systems for the nonlinear Hamiltonian PDEs will be solved by using the simple fixed-point iteration method. For every iteration step, we need to solve linear equations $Ax = b$. Here A is a cyclic matrix, so we can apply FFT for solving the equations.

3 Energy-preserving wavelet collocation method for the NLS equation

The nonlinear Schrödinger equation

$$i\psi_t + \psi_{xx} + a|\psi|^2\psi = 0, \quad a > 0, \tag{3.1}$$

can be written in multi-symplectic form by letting $\psi = p + iq$ and introducing a pair of conjugate momenta $v = p_x$, $w = q_x$ [3]. Separating (3.1) into real and imaginary parts, we obtain the system

$$\begin{cases} q_t - v_x = a(p^2+q^2)p, \\ -p_t - w_x = a(p^2+q^2)q, \\ p_x = v, \\ q_x = w, \end{cases} \tag{3.2}$$

which is equivalent to the multi-symplectic form (2.1) for the NLS equation with

$$\mathrm{z} = \begin{pmatrix} p \\ q \\ v \\ w \end{pmatrix}, \quad \mathbf{M} = \begin{pmatrix} 0 & 1 & 0 & 0 \\ -1 & 0 & 0 & 0 \\ 0 & 0 & 0 & 0 \\ 0 & 0 & 0 & 0 \end{pmatrix}, \quad \mathbf{K} = \begin{pmatrix} 0 & 0 & -1 & 0 \\ 0 & 0 & 0 & -1 \\ 1 & 0 & 0 & 0 \\ 0 & 1 & 0 & 0 \end{pmatrix},$$

and Hamiltonian $S(\mathrm{z}) = \frac{1}{2}\left(v^2 + w^2 + \frac{a}{2}(p^2+q^2)^2\right)$. The corresponding energy and momentum conservation laws are

$$\frac{\partial}{\partial t}\left[\frac{1}{2}\left(\frac{a}{2}(p^2+q^2)^2 - v^2 - w^2\right)\right] + \frac{\partial}{\partial x}(vp_t + wq_t) = 0, \tag{3.3}$$

https://doi.org/10.4208/cicp.231014.110416a Published online by Cambridge University Press

and

$$\frac{\partial}{\partial t}(pw-qv)+\frac{\partial}{\partial x}\left[\frac{a}{2}(p^2+q^2)^2+v^2+w^2-pq_t+qp_t\right]=0. \tag{3.4}$$

Additionally, the NLS equation (3.1) also has local normal conservation law

$$\frac{\partial}{\partial t}\left[\frac{1}{2}(p^2+q^2)\right]+\frac{\partial}{\partial x}(pw-qv)=0.$$

Under periodic boundary conditions, the above local conservation laws can be integrated in x-direction, respectively, to obtain the total energy conservation law

$$\mathcal{E}(t)=\frac{1}{2}\int_0^L\left(\frac{a}{2}(p^2+q^2)^2-v^2-w^2\right)dx=Const,$$

total momentum conservation law

$$\mathcal{I}(t)=\int_0^L(pw-qv)dx=Const,$$

and total normal conservation law

$$\mathcal{N}(t)=\frac{1}{2}\int_0^L(p^2+q^2)dx=Const.$$

Applying the EPWCM (2.19) for the multi-symplectic formulation (3.2) of the NLS equation, we obtain

$$\begin{cases}\frac{Q^{n+1}-Q^n}{\tau}-B_1V^{n+1/2}=a\Big[\Big(\frac{(P^{n+1})^2+(P^n)^2}{2}+\frac{(Q^{n+1})^2+(Q^n)^2}{2}\Big)\bullet\frac{P^{n+1}+P^n}{2}\\ \qquad\qquad+\frac{1}{6}(Q^{n+1}-Q^n)\bullet(P^{n+1}\bullet Q^n-P^n\bullet Q^{n+1})\Big],\\ -\frac{P^{n+1}-P^n}{\tau}-B_1W^{n+1/2}=a\Big[\Big(\frac{(P^{n+1})^2+(P^n)^2}{2}+\frac{(Q^{n+1})^2+(Q^n)^2}{2}\Big)\bullet\frac{Q^{n+1}+Q^n}{2}\\ \qquad\qquad+\frac{1}{6}(P^{n+1}-P^n)\bullet(Q^{n+1}\bullet P^n-Q^n\bullet P^{n+1})\Big],\\ B_1P^{n+1/2}=V^{n+1/2},\\ B_1Q^{n+1/2}=W^{n+1/2}.\end{cases} \tag{3.5}$$

Here τ is the time step, $P^n=(p_0^n,p_1^n,\cdots,p_{N-1}^n)^T$, $P^{n+1/2}=\frac{1}{2}(P^n+P^{n+1})$, $(P^n)^2=P^n\bullet P^n$, $P^n\bullet Q^n=(p_0^nq_0^n,p_1^nq_1^n,\cdots,p_{N-1}^nq_{N-1}^n)^T$, p_l^n is the approximation to $p(x_l,t_n)$, $l=0,1,\cdots,N-1$, etc.

By eliminating the values V and W, and using $\Psi=P+iQ$, the scheme (3.5) is equivalent to

$$i\frac{\Psi^{n+1}-\Psi^n}{\tau}+B_1^2\Psi^{n+1/2}+a\Big\{\frac{|\Psi^{n+1}|^2+|\Psi^n|^2}{2}\bullet\frac{\Psi^{n+1}+\Psi^n}{2}\\ +\frac{1}{6}(\Psi^{n+1}-\Psi^n)\bullet(\Psi^{n+1}\bullet P^n-\Psi^n\bullet P^{n+1})\Big\}=0, \tag{3.6}$$

https://doi.org/10.4208/cicp.231014.110416a Published online by Cambridge University Press

where $P^n=\frac{\Psi^n+\overline{\Psi}^n}{2}$. The residual of LECL for the EPWCM (3.6) is

$$\begin{aligned}
&RE_l=\frac{E_l^{n+1}-E_l^n}{\tau}+(B_1F^{n+1/2})_l,\\
&E_l^n=\frac{1}{2}\left\{\frac{a}{2}\left((p_l^n)^2+(q_l^n)^2\right)^2-(v_l^n)^2-(w_l^n)^2\right\},\\
&F^{n+1/2}=V^{n+1/2}\bullet\frac{P^{n+1}-P^n}{\tau}+W^{n+1/2}\bullet\frac{Q^{n+1}-Q^n}{\tau},
\end{aligned}$$

and the residual of LMCL is

$$\begin{aligned}
&RM_l=\frac{I_l^{n+1}-I_l^n}{\tau}+(B_1G^{n+1/2})_l,\\
&I_l^n=p_l^nw_l^n-q_l^nv_l^n,\\
&G^{n+1/2}=\frac{a}{2}\left((P^{n+1/2})^2+(Q^{n+1/2})^2\right)^2+(V^{n+1/2})^2+(W^{n+1/2})^2\\
&\qquad -P^{n+1/2}\bullet\frac{Q^{n+1}-Q^n}{\tau}+Q^{n+1/2}\bullet\frac{P^{n+1}-P^n}{\tau}.
\end{aligned}$$

Moreover, the discrete total energy is $\mathcal{E}^n=h\sum_{l=0}^{N-1}E_l^n$, the total momentum is $\mathcal{I}^n=h\sum_{l=0}^{N-1}I_l^n$ and the total normal is $\mathcal{N}^n=\frac{1}{2}h\sum_{l=0}^{N-1}\left((p_l^n)^2+(q_l^n)^2\right)$.

4 Energy-preserving wavelet collocation method for the Camassa-Holm equation

The Camassa-Holm (CH) equation

$$u_t-u_{xxt}+3uu_x-2u_xu_{xx}-uu_{xxx}=0, \tag{4.1}$$

is a model equation which represents the unidirectional propagation of shallow water waves over a flat bottom [37]. This equation is rich in geometric structures and is an infinite-dimensional completely integrable Hamiltonian system for a large class of initial data [38]. A great deal of numerical methods have been used to solve the CH equation. Finite difference scheme was proposed and proved to be convergent in [39, 40]. Pseudospectral scheme is used to investigate several aspects of the periodic traveling wave solutions of the CH equation in [38] and the convergence of a spectral projection of the periodic CH equation was given in [41]. A local discontinuous Galerkin method was developed for solving the CH equation in [42]. Recently, David Cohen proposes two new multi-symplectic formulations for the CH equation and make experiments for each formulation by Euler box scheme in [44]. Multi-symplectic wavelet collocation method was proposed for discretizing the CH equation in [27]. In this paper, we propose an energy-preserving wavelet collocation method for the CH equation and simulate the smooth periodic wave and peaked wave solutions.

https://doi.org/10.4208/cicp.231014.110416a Published online by Cambridge University Press

Eq. (4.1) can be rewritten in the form

$$u_t - u_{xxt} - (uu_x)_{xx} + \left(\frac{3}{2}u^2 + \frac{1}{2}u_x^2\right)_x = 0, \tag{4.2}$$

which is equivalent to a multi-symplectic PDEs

$$\begin{cases} \frac{1}{2}\phi_t - \frac{1}{2}p_t - v_x = -w - \frac{3}{2}u^2 - \frac{1}{2}p^2, \\ -\frac{1}{2}u_t + w_x = 0, \\ -\phi_x = -u, \\ u_x = p, \\ \frac{1}{2}u_t = -up + v, \end{cases} \tag{4.3}$$

with $\mathrm{z}=(u,\phi,w,v,p)^T$, Hamiltonian $S(\mathrm{z})=-wu-u^3/2-up^2/2+vp$, and the pair of skew-symmetric matrices **M** and **K**,

$$\mathbf{M}=\begin{pmatrix} 0 & \frac{1}{2} & 0 & 0 & -\frac{1}{2} \\ -\frac{1}{2} & 0 & 0 & 0 & 0 \\ 0 & 0 & 0 & 0 & 0 \\ 0 & 0 & 0 & 0 & 0 \\ \frac{1}{2} & 0 & 0 & 0 & 0 \end{pmatrix}, \quad \mathbf{K}=\begin{pmatrix} 0 & 0 & 0 & -1 & 0 \\ 0 & 0 & 1 & 0 & 0 \\ 0 & -1 & 0 & 0 & 0 \\ 1 & 0 & 0 & 0 & 0 \\ 0 & 0 & 0 & 0 & 0 \end{pmatrix}.$$

The corresponding energy and momentum conservation laws are

$$\frac{\partial}{\partial t}\left(\frac{1}{2}(u^3+uu_x^2)\right) + \frac{\partial}{\partial x}(w\phi_t - vu_t) = 0, \tag{4.4}$$

and

$$\frac{\partial}{\partial t}\left(\frac{1}{2}(u^2+u_x^2)\right) + \frac{\partial}{\partial x}\left(-wu - \frac{1}{2}u^3 - \frac{1}{2}up^2 + vp - \frac{1}{2}pu_t - \frac{1}{2}u\phi_t\right) = 0. \tag{4.5}$$

Under periodic boundary conditions, the above local conservation laws can be integrated in x-direction, respectively, to obtain the total energy conservation law

$$\mathcal{E}(t) = \frac{1}{2}\int (u^3+uu_x^2)dx = Const,$$

and total momentum conservation law

$$\mathcal{I}(t) = \frac{1}{2}\int (u^2+u_x^2)dx = Const.$$

Additionally, the CH equation has a conserved quantity $H_0 = \int u dx$.

https://doi.org/10.4208/cicp.231014.110416a Published online by Cambridge University Press

We apply the wavelet collocation method to discretize the multi-symplectic formulation (4.3) of the CH equation in space and use the AVF method to integrate the semi-discrete system in time. The resulting scheme is

$$\begin{cases} \frac{1}{2}\delta_t\Phi^n-\frac{1}{2}\delta_t P^n-B_1A_tV^n=-A_tW^n-\frac{1}{2}\Big((U^n)^2+U^n\bullet U^{n+1}+(U^{n+1})^2\Big) \\ \qquad\qquad -\frac{1}{6}\Big((P^n)^2+P^n\bullet P^{n+1}+(P^{n+1})^2\Big), \\ \frac{1}{2}\delta_t U^n=B_1A_tW^n, \\ B_1A_t\Phi^n=A_tU^n, \\ B_1A_tU^n=A_tP^n, \\ \frac{1}{2}\delta_t U^n=-\frac{1}{6}(2U^n\bullet P^n+U^n\bullet P^{n+1}+U^{n+1}\bullet P^n+2U^{n+1}\bullet P^{n+1})+A_tV^n, \end{cases} \tag{4.6}$$

where $\delta_t U^n=\frac{U^{n+1}-U^n}{\tau}$ and $A_tU^n=\frac{U^{n+1}+U^n}{2}$, etc. Making initial condition $P^0=B_1U^0$, we have $P^n=B_1U^n$. Eliminating the variables Φ,W,V,P, we can obtain the following EP-WCM for the CH equation (4.2)

$$\begin{aligned} A_t\Big\{&\delta_tU^n-\delta_tB_1^2U^n-\frac{1}{6}B_1^2(2U^n\bullet B_1U^n+U^n\bullet B_1U^{n+1}+U^{n+1}\bullet B_1U^n+2U^{n+1}\bullet B_1U^{n+1}) \\ &+B_1\Big[\frac{1}{2}((U^n)^2+U^n\bullet U^{n+1}+(U^{n+1})^2) \\ &+\frac{1}{6}\Big((B_1U^n)^2+B_1U^n\bullet B_1U^{n+1}+(B_1U^{n+1})^2\Big)\Big]\Big\}=0. \end{aligned} \tag{4.7}$$

Because the scheme (4.7) is a three level scheme, we need a two time levels scheme to give the initial datum for the second level values of the scheme (4.7). Since equation $\phi_x=u$, $u_x=p$ in (4.3) contain no time derivatives, we can omit the operator A_t in the corresponding equations to get more accurate discretizations in (4.6), namely

$$B_1\Phi^n=U^n,\quad B_1U^n=P^n.$$

Then, we can obtain a two time levels scheme for (4.2)

$$\begin{aligned} &\delta_tU^n-\delta_tB_1^2U^n-\frac{1}{6}B_1^2(2U^n\bullet B_1U^n+U^n\bullet B_1U^{n+1}+U^{n+1}\bullet B_1U^n+2U^{n+1}\bullet B_1U^{n+1}) \\ &+B_1\Big[\frac{1}{2}((U^n)^2+U^n\bullet U^{n+1}+(U^{n+1})^2) \\ &+\frac{1}{6}\Big((B_1U^n)^2+B_1U^n\bullet B_1U^{n+1}+(B_1U^{n+1})^2\Big)\Big]=0. \end{aligned} \tag{4.8}$$

https://doi.org/10.4208/cicp.231014.110416a Published online by Cambridge University Press

The three discrete conserved quantities are

$$H_0^n = \sum_{l=0}^{N-1} u_l^n h,$$
$$\mathcal{E}^n = \frac{1}{2}\sum_{l=0}^{N-1} \big((u_l^n)^3 + u_l^n \cdot (B_1 U^n)_l^2\big) h,$$
$$\mathcal{I}^n = \frac{1}{2}\sum_{l=0}^{N-1} \big((u_l^n)^2 + (B_1 U^n)_l^2\big) h.$$

5 Numerical simulation for the NLS equation

For convenience, the EPWCM based on the autocorrelation function of Daubechies scaling function ADM is called EPWCM with ADM (abbr. EPWCM-ADM). To gain insight into the performance of the proposed EPWCM, the following numerical experiments for the NLS equation (3.1) with the constant $a = 2$ are performed. In each time step, the scheme (3.6) is computed by the following fixed-point iteration method

$$i\frac{\Psi^{n+1,(s+1)} - \Psi^n}{\tau} + B_1^2 \frac{\Psi^{n+1,(s+1)} + \Psi^n}{2} + a\Big\{\frac{|\Psi^{n+1,(s)}|^2 + |\Psi^n|^2}{2} \bullet \frac{\Psi^{n+1,(s)} + \Psi^n}{2} + \frac{1}{6}(\Psi^{n+1,(s)} - \Psi^n) \bullet (\Psi^{n+1,(s)} \bullet P^n - \Psi^n \bullet P^{n+1,(s)})\Big\} = 0. \tag{5.1}$$

Taking the initial iteration vector $\Psi^{n+1,(0)} = \Psi^n$, we conduct the iterations until convergence, i.e., when the following criteria is satisfied

$$||\Psi^{n+1,(s+1)} - \Psi^{n+1,(s)}||_2 < 10^{-14}.$$

Here the discrete L^2 and L^∞ norms of complex-valued function ψ are defined as

$$\|\psi\|_2 = \left(h\sum_{l=0}^{N-1} |\psi_l|^2\right)^{1/2} \quad \text{and} \quad \|\psi\|_\infty = \max_{0\le l\le N-1} |\psi_l|.$$

It is noted that the linear equations (5.1) can be solved efficiently by the FFT algorithm. All the simulations are computed by a compiled code of MATLAB 7.1.

Example 5.1. We consider the NLS equation (3.1) with the one-soliton solution

$$\psi(x,t) = \text{sech}\,(x-4t)\exp\left(2i\left(cx - \frac{3}{2}t\right)\right), \tag{5.2}$$

where $c = 1$.

https://doi.org/10.4208/cicp.231014.110416a Published online by Cambridge University Press

Table 1: Space accuracy test of the EPWCM-AD10 for (3.1) with initial condition (5.2) ($\tau=1.0e-6$).

J	N	Error		Order	
		L^∞	L^2	L^∞	L^2
0	100	0.7920	1.5820	-	-
1	200	0.2126	0.3671	1.8977	2.1074
2	400	1.2815e-03	1.6530e-03	7.3739	7.7950
3	800	2.0360e-06	2.4500e-06	9.2979	9.3980
4	1600	2.3527e-09	2.7488e-09	9.7572	9.7998

Table 2: Time accuracy test of the EPWCM-AD10 for (3.1) with initial condition (5.2) ($J=4$, $N=1600$).

τ	Error		Order	
	L^∞	L^2	L^∞	L^2
0.004	1.9223e-04	3.0672e-04	-	-
0.002	4.8052e-05	7.6679e-05	2.0002	2.0000
0.001	1.2013e-05	1.9171e-05	2.0000	1.9999
0.0005	3.0041e-06	4.7941e-06	1.9996	1.9996

Firstly, the problem is solved in $[-50,50]$ till time $t=1$ for accuracy test. The space and time accuracy of the EPWCM (3.6) with AD10 are tested. The L^2 and L^∞ errors and the numerical order of accuracy are given in Tables 1 and 2. Notice that both errors decrease very quickly when the space grid number N becomes larger. As shown in Table 1, the numerical orders measured by the L^∞ error are 1.8977, 7.3739, 9.2979 and 9.7572, which means that the error decays at an exponential rate with respect to the space grid number N. So does the L^2 error. The numerical results are satisfactory, but the error analysis needs to be considered in the future work. Note that in Table 2, the spatial error ($N=1600$) is negligible and the error is dominated by the time discretization error. Table 2 clearly indicates that the AVF method is of second-order in time. Table 3 shows the numerical errors and CPU time of the EPWCM with different ADM. The errors of the EPWCM decrease in an exponential rate in space for each ADM and the decreasing rate is increasing when M becomes larger. Therefore, the EPWCM has high accuracy in space. However, for a fixed grid number N, CPU times used by the EPWCM with different ADM are almost the same little, which is due to the FFT algorithm.

Second, to test the conservation properties of EPWCM, the problem is solved in $[-30,220]$ till time $t=50$ by using the EPWCM-AD10 with grid number $N=1000$ and time step $\tau=0.001$. As can be seen from Fig. 1(a), the motion of the soliton is simulated very well. The errors in global conservation laws are shown in Fig. 1(b)-(d). If the scheme (3.6) is solved exactly, then the total energy is conserved exactly. The global energy is conserved up to the accuracy of the EPWCM, but the errors of the global energy look like to show linear decrease in Fig. 1(c). The following numerical experiments also

https://doi.org/10.4208/cicp.231014.110416a Published online by Cambridge University Press

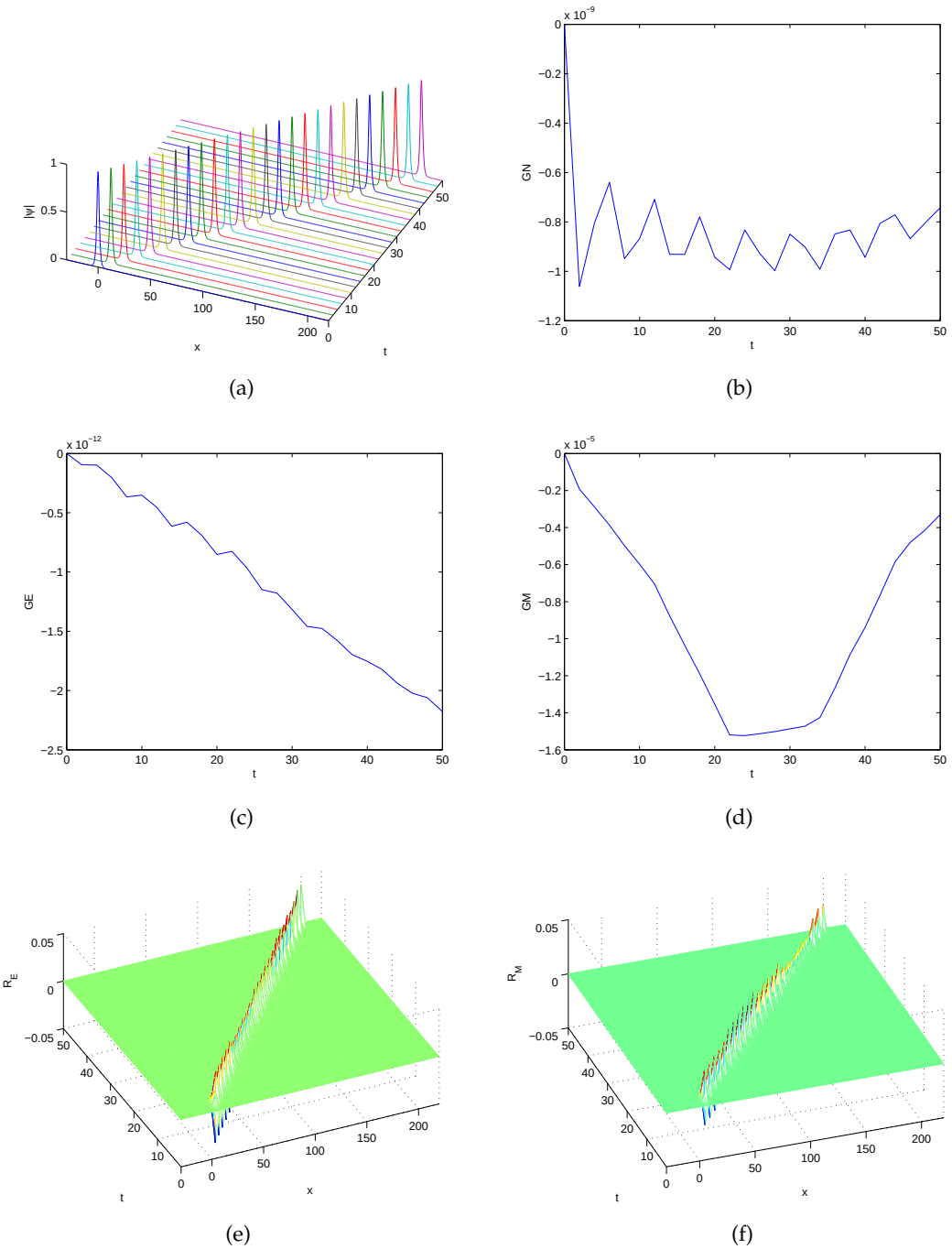


Figure 1: The EPWCM-AD10 ($N=1000$ and $\tau=0.001$) for (3.1) with the initial condition (5.2). (a) Propagation of solitary wave $|\psi|$; (b) error in total norm; (c) error in total energy; (d) error in total momentum; (e) error in LECL; (f) error in LMCL.

https://doi.org/10.4208/cicp.231014.110416a Published online by Cambridge University Press

Table 3: Space accuracy of the EPWCM with AD10, AD20 and AD30 with initial condition (5.2) ($\tau=1.0e-6$, $t=1$).

		EPWCM-AD10	EPWCM-AD20	EPWCM-AD30
$N=200$	L^∞ errors	0.21	5.55e-02	2.54e-02
	L^2 errors	0.37	0.14	8.37e-02
	CPU(s)	392.31	382.84	382.80
$N=400$	L^∞ errors	1.28e-03	2.71e-05	7.11e-06
	L^2 errors	1.65e-03	7.64e-05	3.66e-05
	CPU(s)	769.22	744.58	752.09
$N=800$	L^∞ errors	2.04e-06	7.29e-10	3.98e-11
	L^2 errors	2.45e-06	8.26e-10	1.06e-10
	CPU(s)	1587.94	1591.78	1496.16

appear similar situations. So we suspect that it may be due to solve approximately the discrete nonlinear system by using the iterative method. The residuals in the local conservation laws are also plotted as a function of the spatial grid location and the time step in Fig. 1(e)-(f). The errors are mainly concentrated around the moving front.

Example 5.2. In this example we consider the collision of double solitons of the NLS equation (3.1) with the initial condition [43]

$$\psi(x,0)=\sum_{j=1}^{2}\text{sech}\,(x-x_j)\exp\left(\frac{1}{2}ic_j(x-x_j)\right). \tag{5.3}$$

Here $c_1=4$, $x_1=-10$, $c_2=-4$, $x_2=10$.

For the purpose of numerical, we consider a multi-symplectic wavelet collocation method (MSWCM) [27]. The problem is solved in $[-25,25]$ till time $t=50$ by using the EPWCM-AD10 and MSWCM-AD10 with $N=400$ and $\tau=0.001$. The numerical solutions of the two methods are the same, so we only show the numerical solutions obtained using the EPWCM. As shown in Fig. 2(a), the double solitons collide at $x=\pm 25$ and $x=0$. The shapes and velocities of the double solitons keep unchanged after collision. The numerical errors in the conserved quantities can be found in Fig. 2(b)-(d). It is shown that the EPWCM conserves total energy exactly, while the MSWCM conserves total norm exactly. In this example, the total momentum of the EPWCM is conserved well as that of the MSWCM. These results show that the EPWCM is effective and has good conservation properties.

https://doi.org/10.4208/cicp.231014.110416a Published online by Cambridge University Press

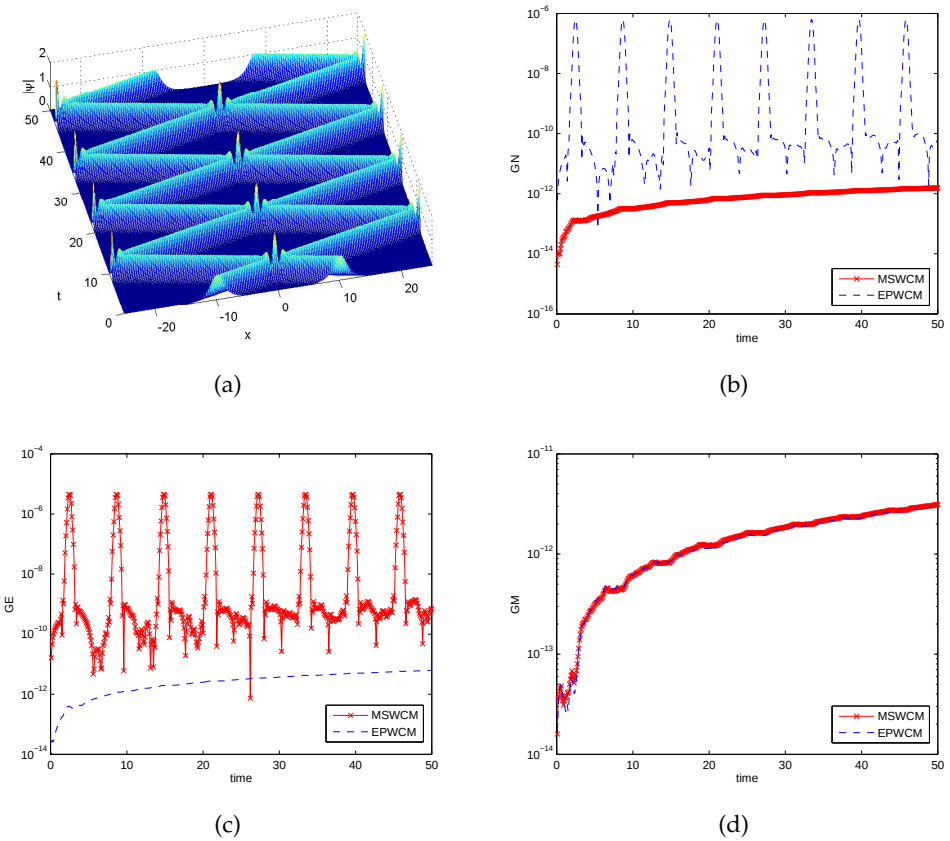


Figure 2: The EPWCM-AD10 and MSWCM-AD10 ($N=400$ and $\tau=0.001$) for (3.1) with the initial condition (5.3). (a) Propagation of solitary wave $|\psi|$; (b) error in total norm; (c) error in total energy; (d) error in total momentum.

6 Numerical simulation for the Camassa-Holm equation

In this section, smooth periodic travelling wave, periodic peakon travelling wave and collision of peakons of the CH equation are simulated in Examples 6.1-6.4. Long time simulations are made for smooth periodic wave in Example 6.1. Accuracy test and long time simulation are made for peakon wave in Example 6.2. Collision of two peakons are given in Example 6.3 and collision of three peakons are given in Example 6.4.

Example 6.1 (Smooth solution). As pointed in [38], the solution of the Camassa-Holm equation can be described by three parameters $m,M,z\in\mathbb{R}$, where $z=c-M-m$. The equation has a smooth periodic travelling wave when three parameters m,M,z fulfill the relation $z<m<M<c$. By choosing $m=0.3$, $M=0.7$ and $c=1$, we study a smooth periodic travelling wave with period of $L\approx 6.56$. The initial data is constructed by performing a spline interpolation to obtain u as a function of x, see [38] for details. Note that the exact

https://doi.org/10.4208/cicp.231014.110416a Published online by Cambridge University Press

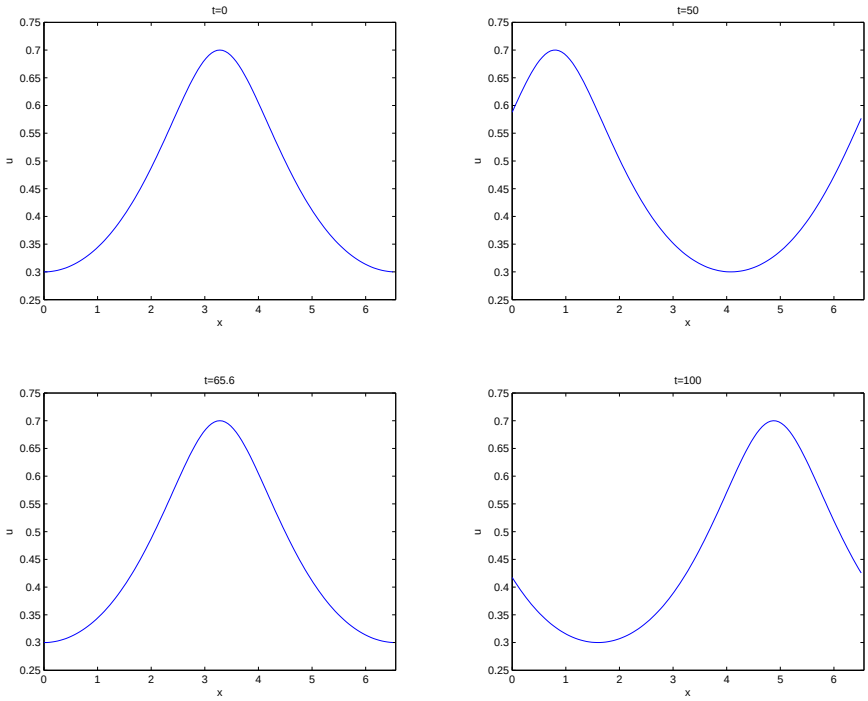


Figure 3: Time evolution of the smooth periodic travelling wave over the time interval $t\in[0,100]$, using the EPWCM-AD10 ($N=128$, $h=0.0512$, $\tau=0.0004$).

solution is obtained by periodic extension of the initial function.

By taking a coordinate transform $x=L\xi$, the CH equation (4.2) is equivalent to

$$u_t-\frac{1}{L^2}u_{\xi\xi t}-\frac{1}{L^3}(uu_\xi)_{\xi\xi}+\frac{1}{L}\left(\frac{3}{2}u^2+\frac{1}{2L^2}u_\xi^2\right)_\xi=0,\quad \xi\in[0,1].$$

Then, the problem is solved till time t=100 by using the EPWCM-AD10 with grid number $N=128$ and time step $\tau=0.0004$. As shown in Fig. 3, the proposed method simulates the smooth periodic travelling wave very well. The L^2 and L^∞ errors at $t=100$ are 1.0371×10^{-5} and 6.1010×10^{-6} respectively. Fig. 4 shows that the invariants are conserved better than the MSWCM (see [27]).

Example 6.2 (Peakon solution). In this example we consider periodic peaked travelling waves with the initial condition

$$u(x,0)=\begin{cases}\frac{c}{\cosh(a/2)}\cosh(x-x_0), & |x-x_0|\le a/2,\\ \frac{c}{\cosh(a/2)}\cosh\big(a-(x-x_0)\big), & |x-x_0|>a/2,\end{cases}\tag{6.1}$$

where c is the wave speed, a is the period and x_0 is the position of the trough.

https://doi.org/10.4208/cicp.231014.110416a Published online by Cambridge University Press

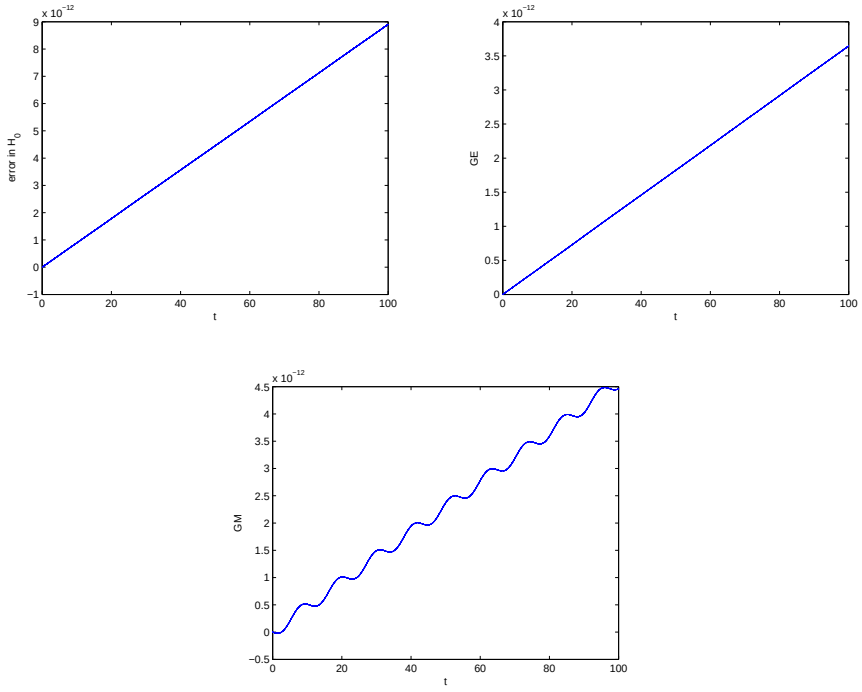


Figure 4: The errors in H0, energy and momentum of the EPWCM-AD10 with the smooth periodic initial data.

Firstly, we present the wave propagation of the CH equation with parameters $c=1$, $a=1$ and $x_0=0$. The computational domain is $[0,a]$. Table 4 shows the numerical errors and CPU time of the EPWCM with different ADM. Compared with the Euler box scheme

Table 4: Space accuracy of the EPWCM with AD10, AD20 and AD30 with initial condition (6.1) (τ=1.0e−5, t=3).

		EPWCM-AD10	EPWCM-AD20	EPWCM-AD30
$N=128$	L^∞ errors	3.02e-03	2.05e-03	1.95e-03
	L^2 errors	5.57e-04	3.54e-04	2.99e-04
	CPU(s)	59.11	59.20	59.16
$N=256$	L^∞ errors	1.53e-03	1.14e-03	9.57e-04
	L^2 errors	2.44e-04	1.40e-04	1.14e-04
	CPU(s)	118.56	118.20	119.64
$N=512$	L^∞ errors	8.39e-04	6.06e-04	5.01e-04
	L^2 errors	1.08e-04	5.68e-05	4.46e-05
	CPU(s)	214.11	218.69	216.38

https://doi.org/10.4208/cicp.231014.110416a Published online by Cambridge University Press

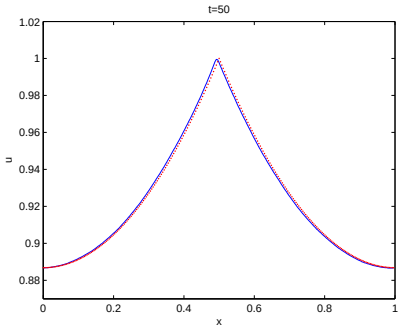


Figure 5: A periodic peakon computed by the EPWCM-AD30 ($N=256$, $\tau=0.0001$). Dashed curves are the initial data while solid curves are computed results.

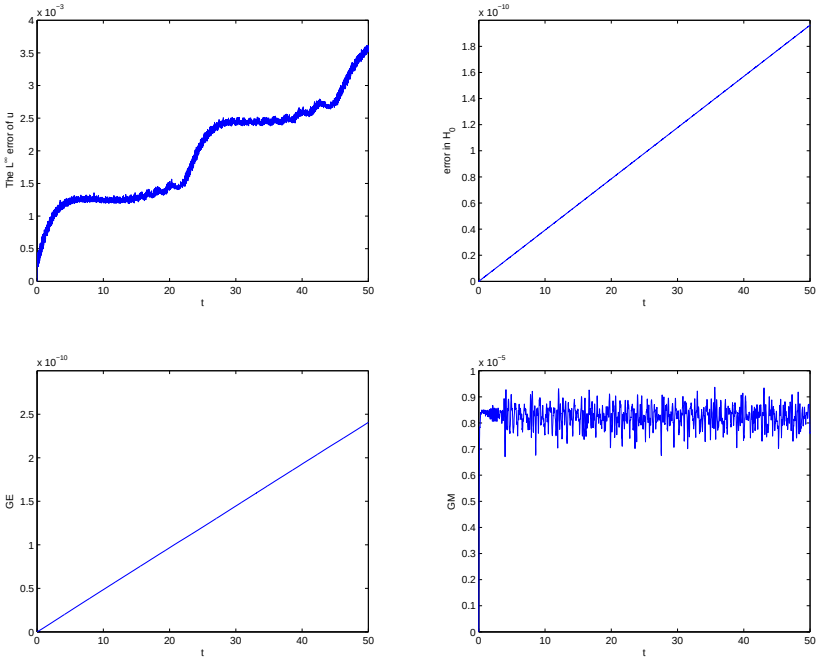


Figure 6: The L^∞ error of numerical solution and the errors in H_0, energy, momentum of the EPWCM-AD30 with the non-smooth periodic initial data (6.1).

in [44] and the spectral method in [41], the errors obtained by the EPWCM are smaller. As the MSWCM in [27], the errors obtained by the EPWCM are the same order of magnitude, but CPU time here is less.

Second, we solve the problem till time $t=50$ by the EPWCM-AD30 with $N=256$ and $\tau=0.0001$. The computed result is shown in Fig. 5. The L^2 and L^∞ errors at $t=50$ are 1.4528×10^{-3} and 3.6188×10^{-3} respectively. The L^∞ error of numerical solution and the errors of invariants are shown in Fig. 6. The errors of H_0, energy, momentum are bounded

https://doi.org/10.4208/cicp.231014.110416a Published online by Cambridge University Press

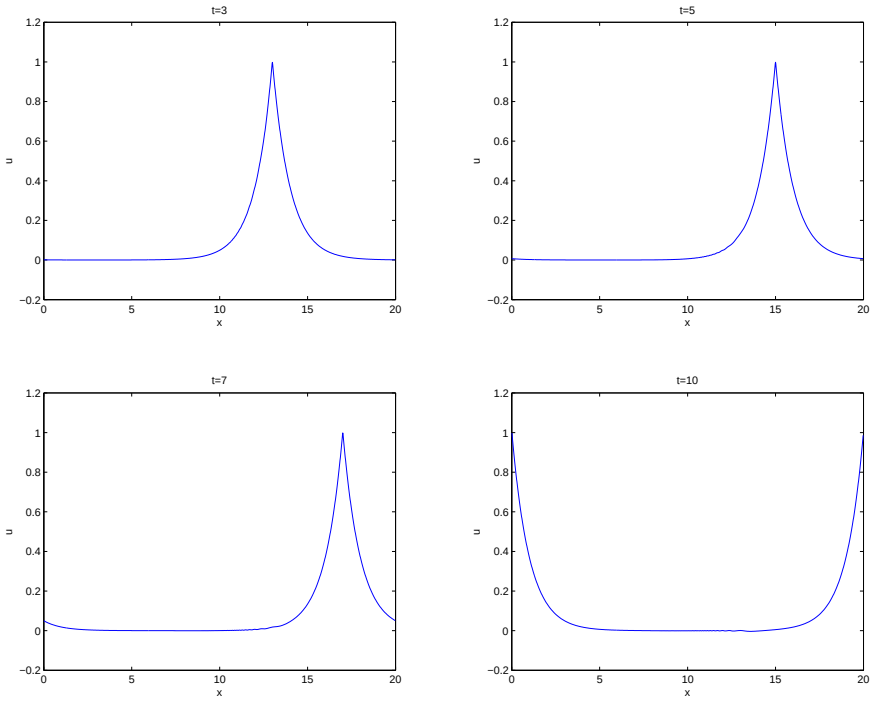


Figure 7: A periodic peakon computed by the EPWCM-AD30 ($N=1280$, $\tau=0.0002$).

by 1.9621×10^{-10}, 2.4064×10^{-10}, 9.3681×10^{-6}, so the invariants are approximately conserved.

Third, we consider the peakon solution with the parameters $c=1$, $a=20$ and $x_0=0$. The problem is solved in $[0,a]$ till time $t=10$ by the EPWCM-AD30 with $N=1280$ and $\tau=0.0002$. As can be seen from Fig. 7, the moving peak profile is resolved very well.

Example 6.3 (Two-peakon interaction). In this example we consider the two-peakon interaction of the CH equation with the initial condition

$$u(x,0)=\phi_1(x)+\phi_2(x), \tag{6.2}$$

where

$$\phi_i(x)=\begin{cases}\frac{c_i}{\cosh(a/2)}\cosh(x-x_i), & |x-x_i|\le a/2,\\ \frac{c_i}{\cosh(a/2)}\cosh\big(a-(x-x_i)\big), & |x-x_i|>a/2,\end{cases}\quad i=1,2. \tag{6.3}$$

The parameters are $c_1=3$, $c_2=1$, $x_1=-8$, $x_2=0$, $a=25$. The computational domain is $[0,a]$. The EPWCM-AD30 is used to simulate this interaction with N=1600 and τ=0.0001. As can be seen from Fig. 8, the taller wave overtakes the shorter one at time $t=4$ and

https://doi.org/10.4208/cicp.231014.110416a Published online by Cambridge University Press

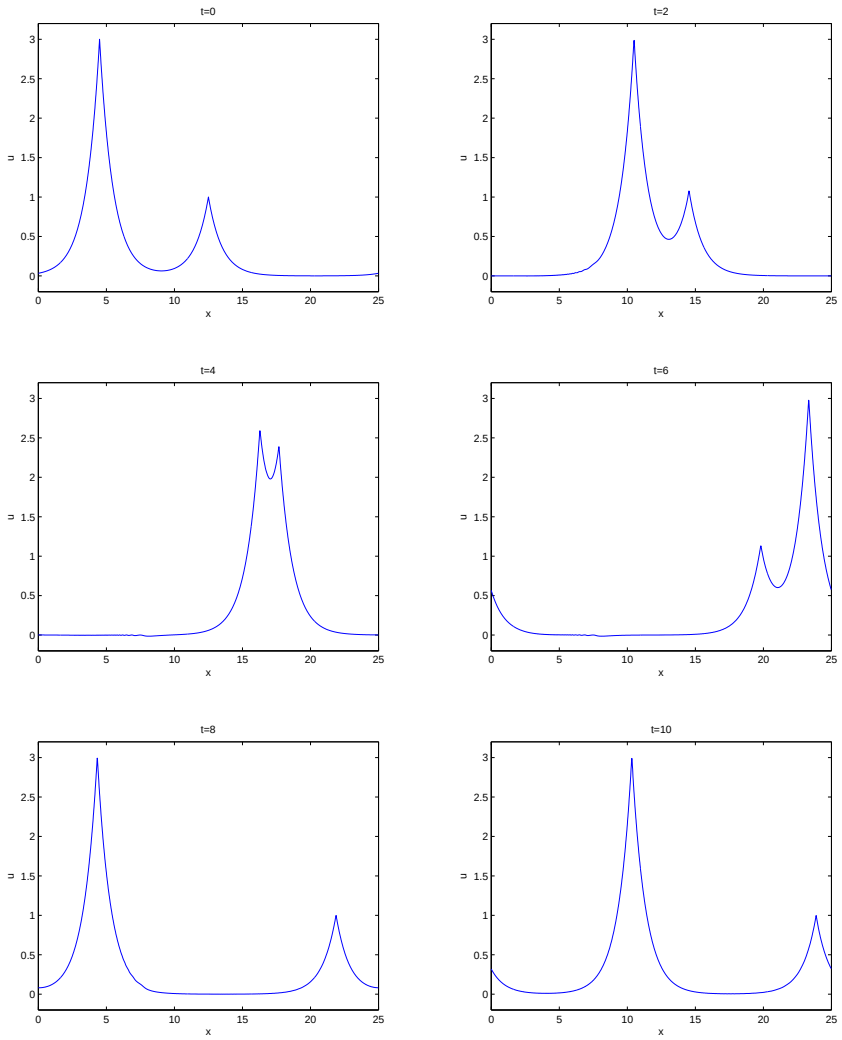


Figure 8: Interaction of two peakons computed by the EPWCM-AD30 ($N=1600$, $\tau=0.0001$).

afterwards both waves retain their original shapes and velocities. The errors of invariants are plotted in Fig. 9. These results show that the EPWCM simulates the interaction of two peakons well.

Example 6.4 (Three-peakon interaction). In this example we show the interaction of three peakons of the CH equation with the initial condition

$$u(x,0)=\phi_1(x)+\phi_2(x)+\phi_3(x), \tag{6.4}$$

where ϕ_i, $i=1,2,3$, are defined as in (6.3). The parameters are $c_1=2$, $c_2=1$, $c_3=0.8$, $x_1=-5$, $x_2=-3$, $x_3=-1$, $a=30$. The computational domain is $[0,a]$. EPWCM-AD30 is used

https://doi.org/10.4208/cicp.231014.110416a Published online by Cambridge University Press

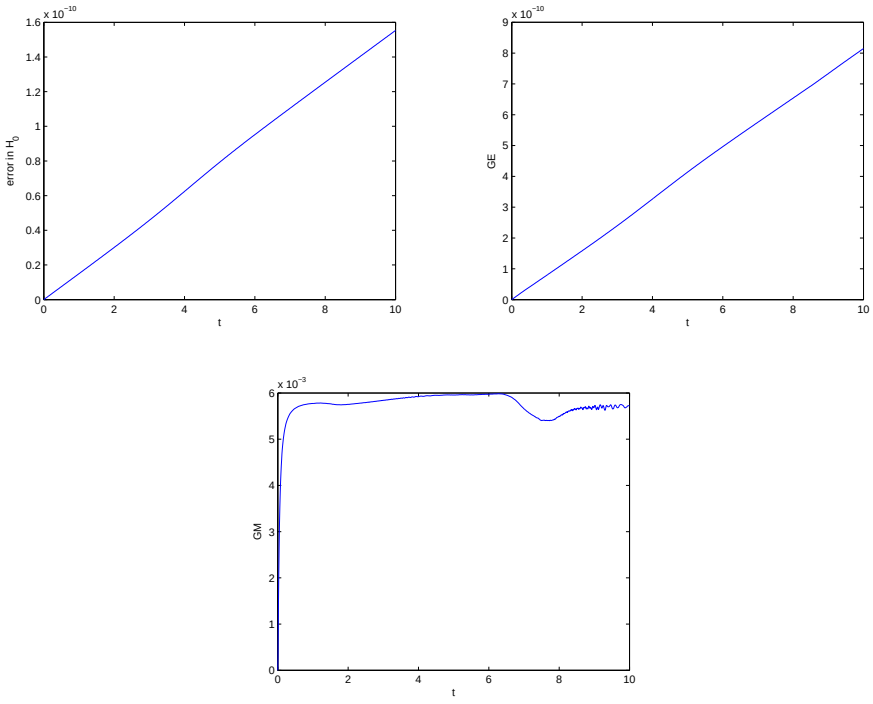


Figure 9: The errors in H0, energy and momentum of the EPWCM-AD30 with the two peakons.

to simulate this interaction with $N=1920$ and $\tau=0.0001$. As can be seen from Fig. 10, the moving peak interaction is resolved very well. In addition, the results obtained here are similar with that obtained by a local discontinuous Galerkin method in [42].

The above numerical results for the CH equation demonstrate the EPWCM can simulate peakons very well and has good conservation properties.

7 Conclusions

In this paper, we develop a novel energy-preserving wavelet collocation method for solving general multi-symplectic formulations of Hamiltonian PDEs with periodic boundary conditions. We apply the proposed method to derive energy-preserving scheme for the NLS and CH equations. Since differentiation matrix obtained by the wavelet collocation method is a cyclic matrix, we can apply Fast Fourier transform to solve equations in numerical calculation. Numerical experiments confirm that the proposed method could conserve energy conservation law and have excellent performance in long time computing. The proposed method can be used for general Hamiltonian PDEs. Therefore, the sine-Gordon equation, the Maxwell's equations and so on can be integrated by the proposed method.

https://doi.org/10.4208/cicp.231014.110416a Published online by Cambridge University Press

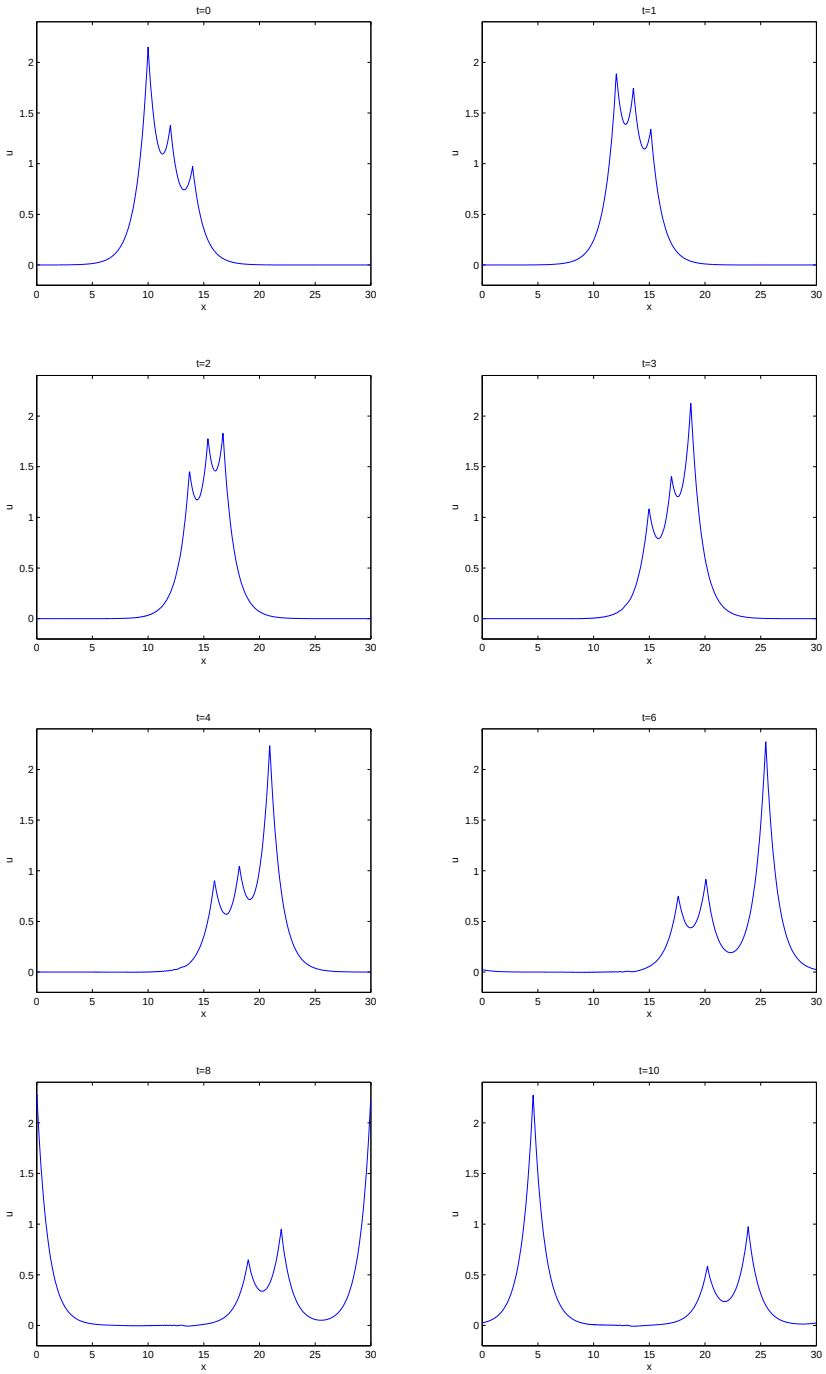


Figure 10: Interaction of three peakons computed by the EPWCM-AD30 ($N=1920$, $\tau=0.0001$).

https://doi.org/10.4208/cicp.231014.110416a Published online by Cambridge University Press

For multi-symplectic Hamiltonian PDEs, the semi-discrete system obtained by discretizing first-order differential operator ∂_x with antisymmetric differential matrix is a large system of Hamiltonian ODEs, which has an energy conservation law. Many methods can be used for spatial discretization, for example Fourier pseudospectral method, wavelet collocation method and compact finite difference method. In this paper, the key of constructing energy-preserving method is to apply a discrete gradient method for the gradient system (2.15). In fact, often the system (2.15) can be written as a energy system $\dot{y} = S\nabla H(y)$ (S is antisymmetric) by eliminating some values. Therefore, one can replace the average vector field method by higher-order energy-preserving B-series method [29], while retaining energy conservation law. It will be considered in the future work.

Acknowledgments

Yuezheng Gong's work is partially supported by China Postdoctoral Science Foundation through Grants 2016M591054. Yushun Wang's work is supported by the Jiangsu Collaborative Innovation Center for Climate Change, the National Natural Science Foundation of China (Grant Nos. 11271195, 41231173) and the Priority Academic Program Development of Jiangsu Higher Education Institutions.

References

[1] E. Hairer, C. Lubich and G. Wanner, Geometric Numerical Integration: Structure Preserving Algorithms for Ordinary Diffenential Equations, Berlin: Springer-Verlag, 2002.
[2] K. Feng and M. Z. Qin, Symplectic Geometric Algorithms for Hamiltonian Systems, Berlin/Hangzhou: Springer-Verlag/Zhejiang Publishing United Group, Zhejiang Science and Technology Publishing House, 2003.
[3] T. J. Bridges, Multi-symplectic structures and wave propagation, Math. Proc. Cambridge Philos. Soc., 121 (1997), 147-190.
[4] J. Marsden, G. Patrick and S. Shkoller, Multi-symplectic Geometry, Variational Integrators and Nonlinear PDEs, Comm. Math. Phys., 199 (1998), 351-395.
[5] S. Reich, Multi-symplectic Runge-Kutta collocation methods for Hamiltonian wave equations, J. Comput. Phys., 157 (2000), 473-499.
[6] S. Reich, Backward error analysis for numerical integrators, SIAM J. Numer. Anal., 36 (1999), 475-491.
[7] J. Frank, B. E. Moore and S. Reich, Linear PDEs and numerical methods that preserve a multi-symplectic conservation law, SIAM J. Sci. Comput., 28 (2006), 260-277.
[8] B. N. Ryland and R. I. Mclachlan, On multi-symplecticity of partitioned Runge-Kutta methods, SIAM J. Sci. Comput., 30 (2008), 1318-1340.
[9] Y. Z. Gong, J. X. Cai and Y. S. Wang, Multi-symplectic Fourier pseudospectral method for the Kawahara equation, Commun. Comput. Phys., 16 (2014), 35-55.
[10] T. J. Bridges and S. Reich, Numerical methods for Hamiltonian PDEs, J. Phys. A: Mathematical and General, 39 (2006), 5287-5320.
[11] Y. S. Wang and J. L. Hong, Multi-symplectic algorithms for Hamiltonian partial differential equations, Comm. Appl. Math. Comput., 27 (2013), 163-230.

https://doi.org/10.4208/cicp.231014.110416a Published online by Cambridge University Press

[12] R. P. Feynman, Conservation of Energy, The Feynman Lectures on Physics, vol. 1, Addison-Wesley Pub. Co., 1965, chapter 4.
[13] T. B. Benjamin, The stability of solitary waves, Proc. Roy. Soc. London A, 23 (1972), 153-183.
[14] S. Li and L. Vu-Quoc, Finite difference calculus invariant structure of a class of algorithms for the nonlinear Klein-Gordon equation, SIAM J. Numer. Anal., 32 (1995), 1839-1875.
[15] B. Y. Guo and L. Vázquez, A numerical scheme for nonlinear Klein-Gordon Equation, J. Appl. Sci., 1 (1983), 25-32.
[16] Z. Fei and L. Vázquez, Two energy conserving numerical schemes for the Sine-Gordon equation, Appl. Math. Comput., 45 (1991), 17-30.
[17] T. D. Ringler, J. Thuburn, J. B. Klemp and W. C. Skamarock, A unified approach to energy conservation and potential vorticity dynamics for arbitrarilystructured C-grids, J. Comput. Phys., 229 (2010), 3065-3090.
[18] Y. Chen, Y. J. Sun and Y. F. Tang, Energy-preserving numerical methods for Landau-Lifshitz equation, J. Phys. A: Math. Theor., 44 (2011), 295207.
[19] J. X. Cai, Y. S. Wang and H. Liang, Local energy-preserving and momentum-preserving algorithms for coupled nonlinear Schröinger system, J. Comput. Phys., 239 (2013), 30-50.
[20] N. Saito and G. Beylkin, Multiresolution repersentations using the autocorrelation functions of compactly supported wavelets, IEEE Trans. Signal Process., 41 (1993), 3584-3590.
[21] O. V. Vasilyev, S. Paolucci and M. Sen, A multilevel wavelet collocation method for solving partial differential equations in a finite domain, J. Comput. Phys., 120 (1995), 33-47.
[22] O. V. Vasilyev and S. Paolucci, A fast adaptive wavelet collocation algorithm for multidimensional PDEs, J. Comput. Phys., 138 (1997), 16-56.
[23] J. W. Ma and H. Z. Yang, Multiresolution symplectic scheme for wave propagation in complex media, Appl. Math. Mech., 25 (2004), 573-579.
[24] J. W. Ma, An exploration of multiresolution symplectic scheme for wave propagation using second-generation wavelets, Phys. Lett. A, 328 (2004), 36-46.
[25] S. Bertoluzza and G. Naldi, A wavelet collocation method for the numerical solution of partial differential equations, Appl. Comput. Harmon. Anal., 3 (1996), 1-9.
[26] H. J. Zhu, L. Y. Tang, S. H. Song, Y. F. Tang and D. S. Wang, Symplectic wavelet collocation method for Hamiltonian wave equations, J. Comput. Phys., 229 (2010), 2550-2572.
[27] H. J. Zhu, S. H. Song and Y. F. Tang, Multi-symplectic wavelet collocation method for the Schrödinger equation and the Camassa-Holm equation, Computer Physics Communications, 182 (2011), 616-627.
[28] R. I. McLachlan, G. R. W. Quispel and N. Robidoux, Geometric integration using discrete gradients, Philos. Trans. R. Soc. A, 357 (1999), 1021-1046.
[29] G. R. W. Quispel and D. I. McLaren, A new class of energy-preserving numerical integration methods, J. Phys. A, 41 (2008), 045206.
[30] E. Celledoni, R. I. McLachlan, D. I. McLaren, B. Owren, G. R. W. Quispel and W. M. Wright, Energy-preserving Runge-Kutta methods, ESAIM: Mathematical Modelling and Numerical Analysis, 43 (2009), 645-649.
[31] E. Hairer, Energy-preserving variant of collocation methods, J. Numer. Anal. Ind. Appl. Math. 5 (2010), 73-84.
[32] E. Celledoni, V. Grimm, R. I. McLachlan, D. I. McLaren, D. O'Neale, B. Owren and G. R. W. Quispel, Preserving energy resp. dissipation in numerical PDEs using the "Average Vector Field" method, J. Comput. Phys., 231 (2012), 6770-6789.
[33] Y. Z. Gong, J. X. Cai and Y. S. Wang, Some new structure-preserving algorithms for general multi-symplectic formulations of Hamiltonian PDEs, J. Comput. Phys., 279 (2014), 80-102.

https://doi.org/10.4208/cicp.231014.110416a Published online by Cambridge University Press

[34] R. M. Gray, Toeplitz and Circulant Matrices: A Review, 2006.
[35] B. Moore and S. Reich, Multisymplectic integration methods for Hamiltonian PDEs, J. Future Gener. Comput. Syst., 19 (2003), 395-402.
[36] J. Wang, A note on multisymplectic Fourier pseudospectral discretization for the nonlinear Schrödinger equation, Appl. Math. Comput., 191 (2007), 31-41.
[37] R. Camassa and D. Holm, An integrable shallow water equation with peaked solitons, Phys. Rev. Lett., 71 (1993), 1661-1664.
[38] H. Kalisch and J. Lenells, Numerical study of traveling-wave solutions for the Camassa-Holm equation, Chaos Solitons Fractals, 25 (2005), 287-298.
[39] G. M. Coclite, K. H. Karlsen and N. H. Risebro, A Convergent Finite Difference Scheme for the Camassa-Holm Equation with General H^1 Initial Data, SIAM J. Numer. Anal., 46 (2008), 1554-1579.
[40] H. Holden and X. Raynaud, Convergence of a finite difference scheme for the Camassa-Holm equation, SIAM J. Numer. Anal., 44 (2006), 1655-1680.
[41] H. Kalisch and X. Raynaud, Convergence of a spectral projection of the Camassa-Holm equation, Numerical Methods for Partial Differential Equations, 22 (2006), 1197-1215.
[42] Y. Xu and C. W. Shu, A local discontinuous Galerkin method for the Camassa-Holm equation, SIAM J. Numer. Anal., 46 (2008), 1998-2021.
[43] Y. Xu and C. W. Shu, Local discontinuous Galerkin methods for nonlinear Schrödinger equations, J. Comput. Phys., 205 (2005), 72-97.
[44] D. Cohen, B. Owren and X. Raynaud, Multi-symplectic integration of the Camassa-Holm equation, J. Comput. Phys., 227 (2008), 5492-5512.

https://doi.org/10.4208/cicp.231014.110416a Published online by Cambridge University Press